Biochemical and Biophysical Research Communications 425 (2012) 485–492

Contents lists available at SciVerse ScienceDirect

Biochemical and Biophysical Research Communications

journal homepage: www.elsevier.com/locate/ybbrc

Structural properties of metal-free apometallothioneins

Kelly L. Summers [a], AnjanPreet K. Mahrok [b], Michael D.M. Dryden [b], Martin J. Stillman [a,b,*]

[a] Department of Biology, The University of Western Ontario, London, Ontario, Canada N6A 5B7
[b] Department of Chemistry, The University of Western Ontario, London, Ontario, Canada N6A 5B7

ARTICLE INFO

Article history:
Received 20 July 2012
Available online 1 August 2012

Keywords:
Apometallothionein
Zinc metallothionein
Electrospray ionization mass spectrometry
Protein folding
Protein structure
Molecular dynamics
Parabenzoquinone

ABSTRACT

The metalated forms of metallothionein are well studied (particularly Zn–MT, Cu–MT and Cd–MT), but almost nothing is known about the chemical and structural properties of apometallothioneins despite their importance in initial metalation and subsequent demetalation. Electrospray ionization mass spectrometry was used to provide a detailed view of the structural properties of the metal-free protein. Mass spectra of Zn_7–MT and apo-MT at pH 7 exhibit the same charge state distribution, indicating that apo-MT is tightly folded like the metallated protein, whereas apo-MT at pH 3 exhibits a charge state spectrum associated with unfolding or denaturation. Benzoquinone was used to modify the cysteines in the β-MT (9 Bq), and α-MT (11 Bq) fragments, and the full βα-MT (20 Bq) protein. ESI-MS showed that the overall volume and, therefore, the extent of folding for the modified proteins is similar to that of Zn–MT. Molecular modeling using MM3-MD methods provided the volume of each modified protein. The volumes of the partially modified proteins follow the same trend as the charge states, showing that ESI-MS is an excellent method with which to follow small changes in protein folding as a function of applied chemical stress. The data suggest that the structure of apo-βα-MT is more organized than previously considered.

1. Introduction

Since horse liver metallothionein was first described in 1957 [1] the emphasis of reported research has been on the metalation properties of the protein. Metalation *in vitro* can be from either the metal-free apoprotein [2–4] or from a metalated protein bound to metals with a lower binding affinity [5,6]. For example, many metals will displace Zn^{2+} either isomorphously (Cd^{2+}) [7] or by a change in structure (Cu^{+}) [8]. The metalation reaction is quite different for the apoprotein compared with the Zn- or Cd-saturated proteins often used for *in vitro* studies. The holoprotein is used as the starting point because the 20 thiols are protected from oxidation, especially near neutral pH when the sulfurs are particularly vulnerable, and because the cellular chemistry of, for example, Cd^{2+} binding by liver metallothioneins would probably occur by displacement of Zn^{2+}.

The initial posttranslational metalation of metallothioneins requires the metal-free protein. Despite binding up to seven divalent metals, particularly the biologically relevant Zn^{2+}, the sequence of events leading to complete metalation of MT is unknown. The experimental issues for monitoring the stepwise metalation of 7 Zn^{2+} for the full, apo-βα-MT are substantial even excluding the problems introduced by the 20 oxygen-sensitive thiols. Neither the apoprotein nor the Zn^{2+} offer good spectroscopic probes as the protein is devoid of aromatic residues and the Zn^{2+} is essentially colorless optically and by NMR spectroscopy.

Rigby et al. reported detailed molecular modeling studies of both the apoprotein and partially metallated proteins from which it was proposed that the structure of the apoprotein at neutral pH was folded so that the thiols were exposed on the surface of a spherical protein [9–12]. The structure could still be called a random coil due to its fluxionality and lack of significant CD signal in the structural region (180–230 nm); however, this proposal was experimentally difficult to support.

Clearly, further studies of the apometallothioneins were needed and we report here experimental structural data for the apoprotein based on changes in the charge state distribution in the electrospray ionization mass spectra as a function of modifications of the cysteinyl thiols. Using four experimental conditions we challenged the structure of apometallothionein. We used ESI-MS as a means of interrogating structural changes. We include detailed molecular dynamics calculations that, together with the experimental data, provide firm evidence for the structure of the metal-free protein. The chemistry reported can also be used to determine the number of free cysteines in a partially metallated protein.

2. Materials and methods

The expression and purification methods have been previously reported [13]. β-rhMT 1a, α-rhMT 1a and βα-rhMT 1a proteins

* Corresponding author at: Department of Chemistry, The University of Western Ontario, London, Ontario, Canada N6A 5B7.
E-mail address: martin.stillman@uwo.ca (M.J. Stillman).

0006-291X/$ - see front matter © 2012 Elsevier Inc. All rights reserved.
http://dx.doi.org/10.1016/j.bbrc.2012.07.141

used in this study were based on the 38-residue, 43-residue, and 72-residue sequences, respectively: β-rhMT 1a MGKAAAACSC ATGGSCTCTG SCKCKECKCN SCKKAAAA, α-rhMT 1a GSMGKAAAAC CSCCPMSCAK CAQGCVCKGA SEKCSCCKKA AAA, βα-rhMT 1a MGKAAAACSC ATGGSCTCTG SCKCKECKCN SCKKAAAACC SCCPMSCAKC AQGCVCKGAS EKCSCCK KAA AA. In this paper "rhMT" refers to the 1a isoform. There are 9, 11, and 20 cysteine residues present in β-rhMT, α-rhMT and βα-rhMT, respectively, and no aromatic residues or disulfide bonds. The expression system included an N-terminal S-tag (MKETAAAKFE RQHMDSPDLG TLVPRGS) for stability [14,15]. Recombinant β- and α-rhMT were expressed in BL21(DE3) *Escherichia coli* while βα-rhMT was expressed in ER2566 *E. coli*. Both cell lines were transformed using the pET29a plasmid. The S-tag was removed using a Thrombin CleanCleave™ Kit (Sigma). To impede oxidation of the cysteine residues to disulfide bonds, protein samples were argon saturated and rigorously evacuated. Concentrated HCl (Caledon Laboratory Chemicals) was used to demetalate protein samples, followed by desalting on a G-25 (Sephadex) column.

Solutions of 500 mM parabenzoquinone (Bq; Fisher Scientific) were prepared in 100% methanol (Caledon Laboratory Chemicals) and diluted to 50 mM in >16 MΩ cm deionized water (Barnstead Nanopure Infinity). Bq solutions were bubbled extensively with argon. The reaction of benzoquinone with thiols has been previously described [16].

Protein solutions were prepared in pH 2.7 HCOOH (Caledon Laboratory Chemicals) for ESI-MS studies. Protein concentrations were determined by remetalation with Cd^{2+} and examination of the UV–visible absorption spectrum at 250 nm, which corresponds to the ligand-to-metal charge transfer transition generated by the metal-thiolate bond ($\varepsilon_{\beta 250}$ = 36,000 $M^{-1}cm^{-1}$; $\varepsilon_{\alpha 250}$ = 45,000 $M^{-1}cm^{-1}$; $\varepsilon_{\beta\alpha 250}$ = 89,000 $M^{-1}cm^{-1}$). For ESI-MS protein solutions, the pH was adjusted using NH_4OH (Caledon Laboratory Chemicals) and HCOOH (Caledon Laboratory Chemicals).

Mass spectra were collected on a micrOTOF II electrospray-ionization time-of-flight mass spectrometer (Bruker Daltonics, Toronto, Ontario, Canada) in the positive ion mode. NaI was used as the mass calibrant. The scan conditions for the spectrometer were: end plate offset, −500 V; capillary, +4200 V; nebulizer, 2.0 bar; dry gas flow, 8.0 L/min; dry temperature, 30 °C; capillary exit, 180 V; skimmer 1, 22.0 V; hexapole 1, 22.5 V; hexapole RF, 600 Vpp; skimmer 2, 22 V; lens 1 transfer, 88 μs; lens 1 pre puls storage 23 μs. The range was 500.0–3000.0 m/z, averaging 2 × 0.5 Hz. Spectra were constructed and deconvoluted using the Bruker Compass DataAnalysis software package.

Molecular modeling calculations were conducted using Scigress Version 3.0.0 (Fujitsu Poland Ltd.) operating on Intel® Core™ i7 PCs with 8 GB RAM. Modelling parameters and sequence information have been previously described by Rigby and Stillman [9].

3. Results and discussion

The experiments presented here use the sensitivity of the ESI-MS charge states to indicate changes in protein volume, which are based on folded structure as a function of applied chemistries. The conventional method to change the folding of a protein is to denature it. For apometallothioneins this is not quite as straightforward because the 2° structure of MT is largely based on metal-induced folding, such that in the absence of metalation the apoprotein is often referred to as a random-coil. The modeling studies of Rigby-Duncan et al. suggested the apoprotein is loosely folded and the overall structure of the apoprotein at neutral pH is more like the tightly folded metalated form than the expected open, denatured conformation [9–12]. The actual structure of the metal-free protein impacts both the rate and mechanism of metalation (related to MT function), and the accessibility of the 20 thiols to oxidation. In a loose, denatured conformation one might expect the 20 cysteines to be directly exposed to the solvent and, therefore, prone to oxidation; whereas in a tighter conformation the cysteines might be protected and, therefore, resist oxidation. The difficulty is in probing the structure of a peptide chain that is highly fluxional and does not include chromophorically useful residues. We used the change in charge states as a function of acidity and cysteine modification coupled with molecular modeling to provide images of structures that might exhibit the experimental data.

3.1. Metal-free and metalated metallothionein are similarly folded at neutral pH but unfolded at acidic pH

The folded structure for Zn_7–MT has been deduced from 2D-^{1}H NMR [17] and is identical to that of Cd_7–MT; a species for which X-ray [18], Cd-NMR [17,19,20], EXAFS [21–23] and modeling methods [24,25] all agree is a tight, dumb-bell structure dominated by Cd-thiolate cross-linking [26]. The high resolution ESI-MS provides a new tool with which to study the structures of solutions: the charge state distributions. It is conventional wisdom that if the solution conditions are similar (same salt buffer and concentration), the charge state manifold provides information on the surface area that supports the charge [27,28]. The charge states are dependent on both accessible basic and, therefore, protonatable amino acids and the approximate surface area (or volume) that allows for the spatial separation of the charges on each molecule following dehydration during ionization in the MS [29,30].

Fig. 1 shows the charge state mass spectra for the three significant species in metallothionein chemistry: the metal-free apoprotein at pH 7, the fully metallated holoprotein at pH 7, and the apoprotein at pH 3. The low pH data (Fig. 1F) shows that a single zinc atom remains. There is also a slight zinc contamination at pH 7. It has been reported by Blindauer and coworkers that the last zinc bound to MT is difficult to remove [31]. The contamination does not alter the interpretation because the ESI-MS data show the charge states for each species and we can exclude the zinc-containing species from our analysis.

The charge state distribution data in Fig. 1(A–C) provide significant information about the structures of the apo- and holo-proteins. The distributions for Zn_7- (B) and apo-βα-rhMT (A) at neutral pH are almost identical. The expected normal distribution of the charge state manifold, observed from 3+ to 8+ with a maximum of 5+, initially identifies a constrained structure with minimal surface area, which must be globular in nature to reduce the surface area of the 68 amino acid chain. Molecular modeling of the M_7-MT [12,13] suggests that unlike the solid-state X-ray structure (of rat liver Cd_5Zn_2–MT) [20], which exhibits a well-formed two-domain shape, the domains essentially coalesce in solution (Fig. 4).

There is a slight – but significant – difference in the charge state manifold for the holoprotein (Fig. 1B) compared with the apoprotein at pH 7 (A), which could result from a structure that is slightly larger because the 3+ and 4+ states decrease and the 6+ increases in magnitude. This is reasonable in view of molecular dynamics calculations by Rigby and Stillman, which predicted a tight, globular structure for apoMT compared with the two coalesced but distinct metal-binding domains in the holoprotein [9].

Fig. 1(C and F) show the mass spectra for apo-βα-MT at low pH. Typically, acidic conditions denature proteins, which we associate with an increase in surface area and loss of folding (i.e. pH-induced denaturation of myoglobin [32]). The low pH charge state spectrum (C) is quite different compared with the pH 7 data (A). The charge state manifold has a maximum at 8+ and significant intensity in the 9+ charge state. Clearly, the protein is unfolded. Because

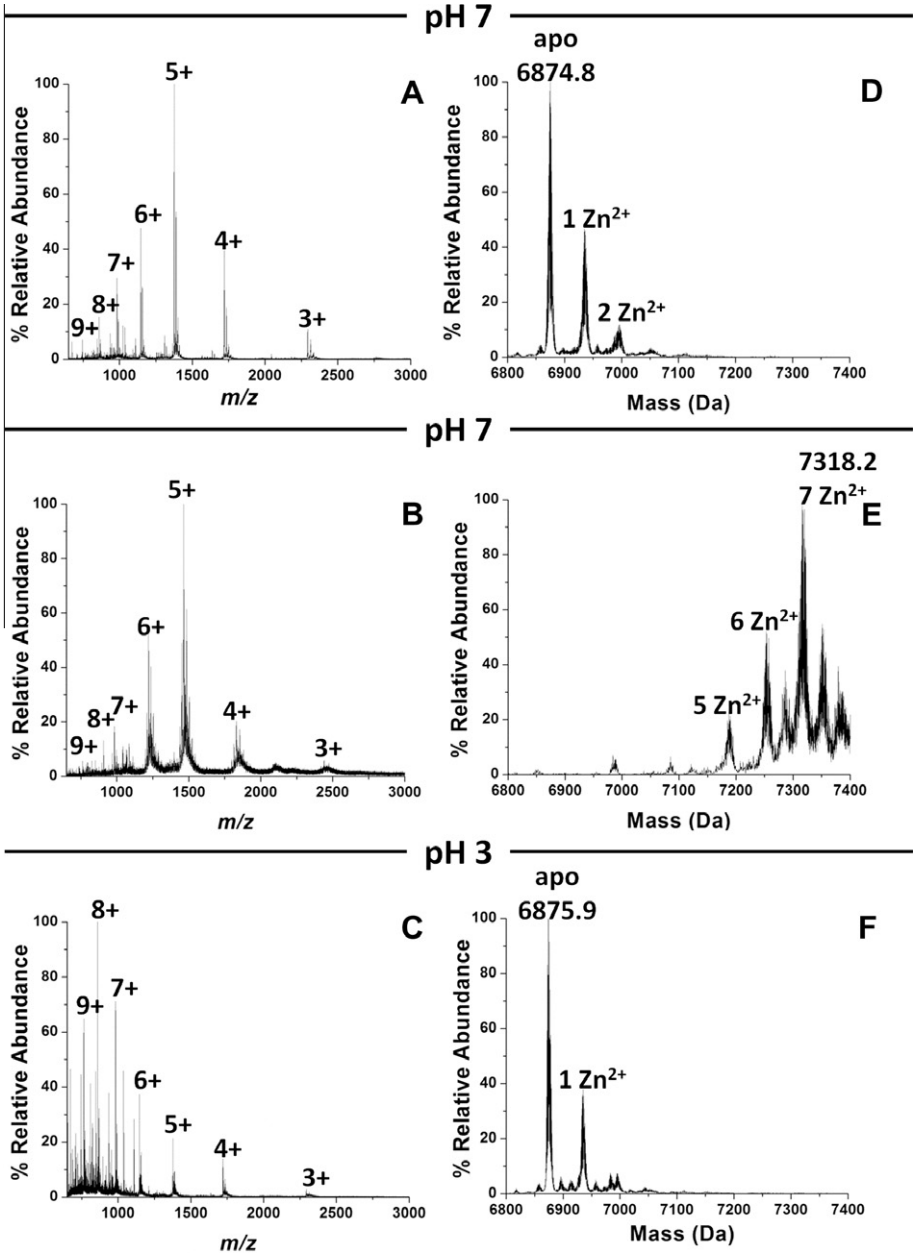

Fig. 1. ESI-MS recorded for rhMT 1a. (A) Charge state spectrum for apo-rhMT at pH 7. (D) The deconvoluted spectrum from (A), showing the mass as 6874.8 Da with a slight Zn^{2+} impurity. (B) Charge state spectrum for Zn_7-rhMT at pH 7. (E) Deconvoluted spectrum from (B) showing the mass of Zn_7-rhMT as 7318.2 Da. (C) Charge state spectrum of metal-free rhMT at pH 3. (F) The deconvoluted spectrum from (C) showing the mass of apo-hMT is 6875.9 Da following acid-induced demetalation.

metallothioneins exhibit very little 2° structure it is confusing to say the protein is denatured under these conditions. From previous studies titrating with Cd^{2+} we believe the pH has to be below 1 to make the protein unable to bind metals [13,15,33]. There was a conformation that resisted metalation as the pH was raised so that two conformations coexisted at intermediate pH values. Essentially, the 2° and 3° structure for MT arises from metal-induced folding [9,10,12].

While the increase in charge state maximum is an important determinant of structural change, the similarity in the charge state maxima of Zn_7–MT and apo-MT measured at pH 7 in Fig. 1 is also significant. The lack of change supports the proposal of Rigby and Stillman that the apo-MT structure is close in overall volume to the tight structure of the metallated protein [9]. The data in Fig. 1 provide important information about the metal-free structure of MT, a vital structure that is almost impossible to describe by the usual structural tools. Data in recent papers were interpreted to show that the metalation process for Zn^{2+} and As^{3+} proceeded in a series of bimolecular reactions initially forming 1 ZnS_4 unit then increasing sequentially up to 5 ZnS_4 units before cluster formation with the 6th and 7th metals [34,36]. The incoming metals initially bind the most exposed thiols, but because the structure of apo-MT is currently unknown, modeling cannot be used to suggest appropriate mutations to identify the site of initial metalation.

3.2. Benzoquinone modifications to the cysteines show that the structure is the same as the metalated protein at pH 7

Bq cysteine modifications allow the structural properties of the metal-free protein and its fragments to be compared with apo-MT near neutral pH.

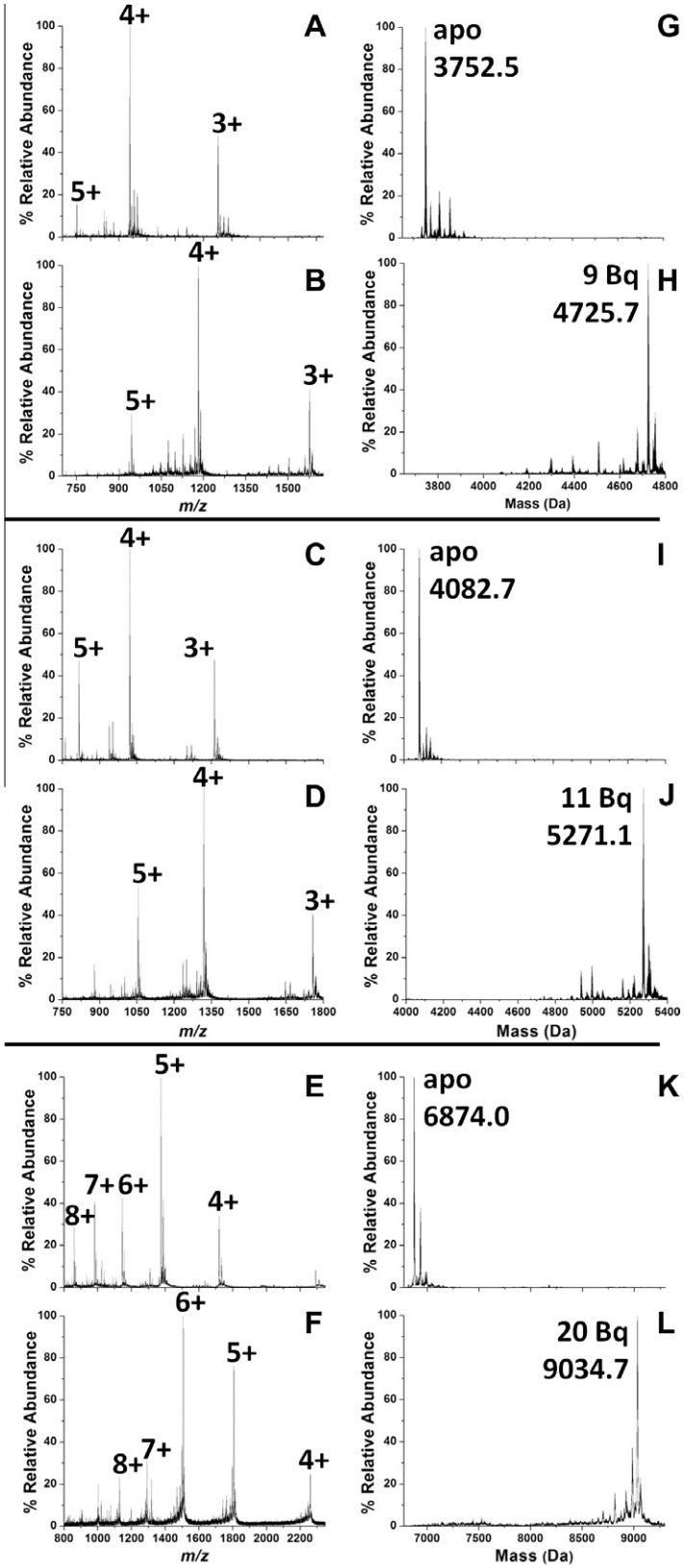

Fig. 2. ESI-MS measured at pH 5.5 showing the complete coupling of Bq to the cysteines in the metal-free β- and α- fragments and the full apo-βα-rhMT 1a. Spectra on the left (A–F) show the charge state distributions. The corresponding deconvoluted data on the right (G–L) present the observed masses for β-, α-, and βα-hMT, respectively. (A and G), (C and I), and (E and K) include spectra of the apo proteins (B and H), (D and J), and (F and L) show the spectra for the domain fragments and the full protein when all the cysteines (9, 11, and 20, respectively) are bound by Bq.

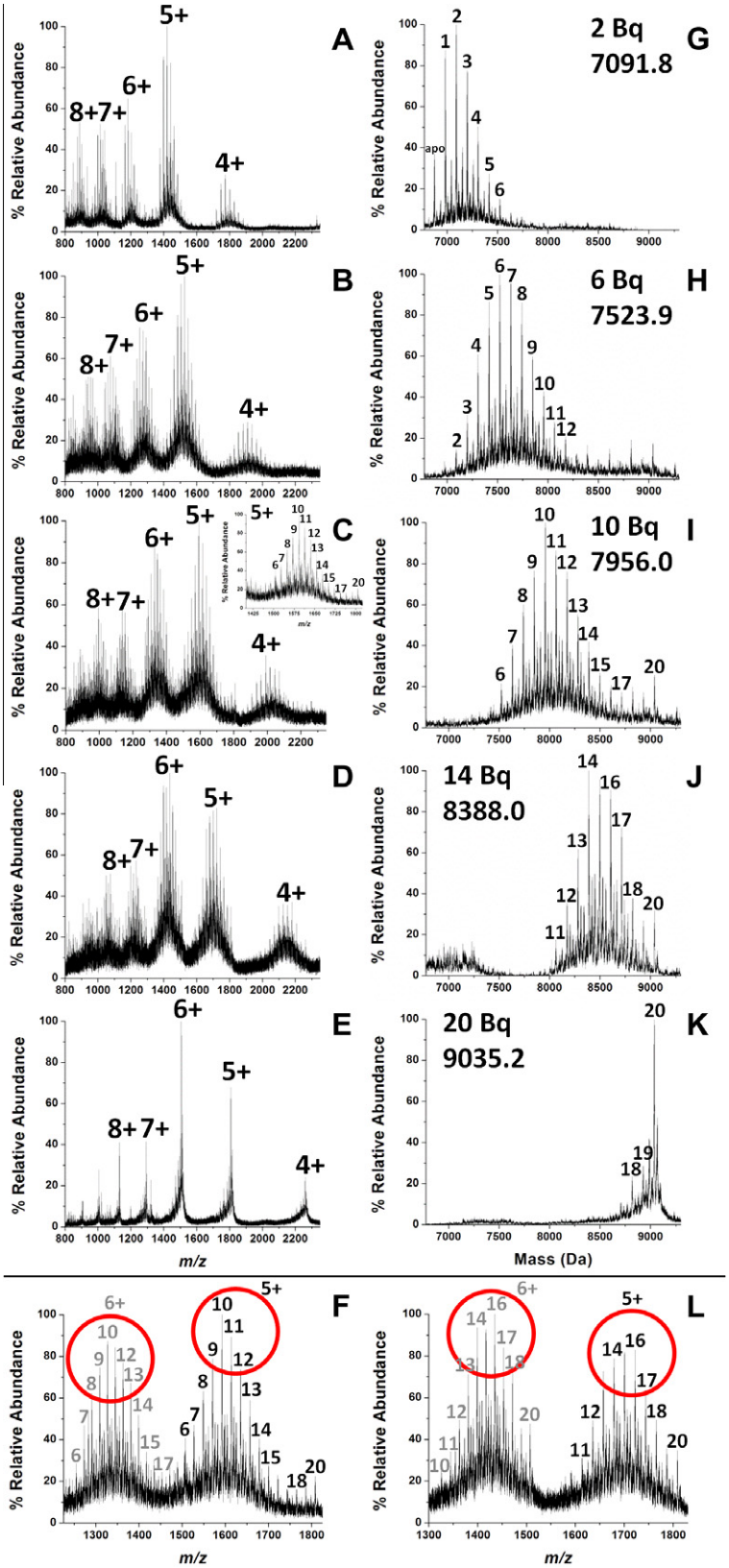

Fig. 3. ESI-MS showing five stages in the complete coupling of all 20 cysteines in apo-βα-rhMT 1 to Bq as aliquots were added at pH 5.5 (A–K). Bq modifies the cysteine adding 108.09 Da to the mass of the protein each time. (F and L) The 5+ and 6+ charge states as a function of Bq loading; (F) average 11 Bq; (L) average 16 Bq. The 5+ charge state diminishes at the expense of the 6+ charge state beginning with 12 Bq.

The deconvoluted spectra for the cysteine-modified species in Fig. 2(H, J, and L) show that 9 Bq added to the β fragment modified the 9 cysteines, 11 Bq modified the 11 cysteines of the α fragment and 20 Bq modified the 20 cysteines of the full protein. Bq modifies each cysteine adding 108.09 Da to the mass of the protein. The more important information is contained in the charge state spec-

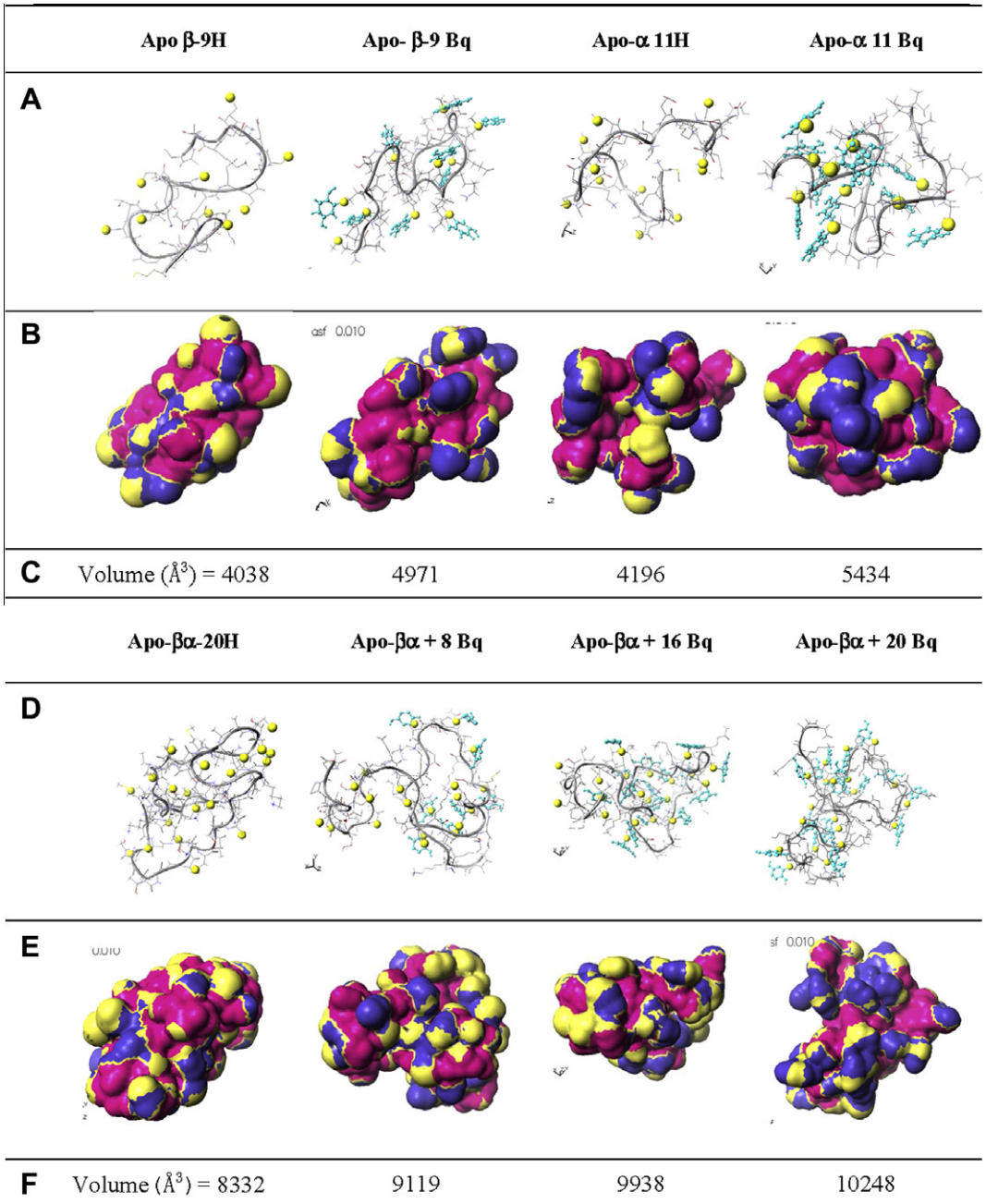

Fig. 4. Calculated protonated and Bq-saturated structures for α-, β- and βα-MT from a molecular dynamics (MM3/MD) calculation for 5000 ps. Internal volume calculations are shown for each. (D and E) show the calculations for the consecutive addition of 8, 16, and 20 Bq cysteine modifiers. Each structure was calculated using MM3/MD methods for 5000 ps. Bq is colored cyan and the cysteines are yellow spheres.

tra shown in Fig. 2(B, D, and F). The charge state manifold for each species shows a slight increase in average charge; for example, compare the relative magnitudes of the 5+/4+/3+ manifold of states between (A) and (B) for the β-fragment, and between (C) and (D) for the α-fragment. There is a more significant increase in the charge state average between (E) and (F) for the full protein with the manifold maximum increasing from 5+ to 6+.

These ESI-MS charge state data are revealing: the modified fragments clearly wrap as tightly as the native peptide. The 20-cysteine full protein expands somewhat with the 6+ charge state intensifying compared with the 5+ state of the 20(SH)apo-MT. This is not unexpected when one considers the structural constraints in folding the peptide chain with 20 Bq tagged to the 20 cysteines. We investigated the change in volume of the protein as a function of Bq modification by adding the Bq in aliquots. Because each species exhibits its own set of charge states independently of other species in the solution we can probe the change in volume of the protein as a function of each addition from 1 to 20 (Fig. 3).

As the mole fraction of Bq added to apo-βα-rhMT increases, the Bq couples to form a normal distribution of up to 10 species until the maximum is reached (Fig. 3(E and K)). While the charge state data are complicated, the deconvolution provides a clearer description of the incremental modification of the cysteines. The interest in this titration with respect to the structure of apo-MT is to determine at what point the charge state maximum changes. Clearly the 5+ charge state is more intense than the 6+ for 1 Bq to approxi-

mately 11 Bq and 6+ is greater than 5+ for 12 to 20 Bq. Fig. 3(F and L) shows the charge state data labeled to indicate the Bq loading of the apo-βα-rhMT.

3.3. Charge states show that apo-MT only slightly expands even when 20 Bq are bound

A close up of the transition from 5+ to 6+ as the most abundant charge state is shown as a function of the Bq loading in Fig. 3(F and L).

A comparison of the charge state distributions of apo-βα-rhMT at low pH and Zn_7-βα-rhMT MT at pH 7 (Fig. 1), and the Bq_{20}-apo-βα-rhMT at pH 5.5 (Fig. 2) suggests that while there is expansion at the 12 Bq point (Fig. 3(F and L)), overall there is little change in the protein volume between the apo-βα-rhMT, the Zn_7-βα-rhMT, and the fully modified Bq_{20}-apo-βα-rhMT. Fig. 3(F and L) allows the details of the increase in volume to be determined more precisely.

To test the reasonableness of the interpretation of the MS data, we carried out a series of molecular dynamics calculations to model the structures that might exist for the Bq-saturated isolated α-, and β-domains and the full βα-MT protein. Using the NIH calculator [35] we determined the volume for each structure. Fig. 4(A) compares the protonated and Bq saturated structures for β- and α-rhMT following molecular dynamics calculations for 5000 ps. The results show that although the backbone ribbon changes location it retains a tightly wrapped structure. Fig. 4(B) shows the volumes of the modeled structures calculated according to NIH methods. The two Bq-saturated fragments clearly maintain a structure similar to that of the apo-fragments at pH 7. Fig. 4(D and E) also show three calculations for the sequential addition of 6, 14 and 20 Bq to the full protein to test for the change in volume as a function of Bq loading. The backbone ribbon clearly shows that while the folded, tight structure is maintained, the structure is clearly larger when 20 Bq are bound. The calculated volume can be compared with the experimental charge state data for both the apo- and Bq-saturated-apo isolated domains and the full protein.

Considering the experimental data we find that the charge state maximum for apo-βα-MT is 5+ whereas the maximum for Bq_{20}-βα-MT is 6+ (Fig. 2). The charge state manifolds for the two metal-free fragments at pH 5.5 is 4+. The charge states show a slight increase in the 5+ and a decrease in the 3+ state when the cysteines in the two fragments are modified by Bq. The volume calculations of Fig. 4(C) more or less track this trend with an approximately 25% increase between the apo- and modified apo structures. For βα-MT we show more detailed changes in the charge states in Fig. 3. As the total amount of Bq added to apo-βα-MT increases, the average number of Bq bound increases as shown in Fig. 3. The 6+ predominates with greater than 12 Bq bound, so that with 16 Bq bound the 6+ is clearly more intense than the 5+ state (Fig. 3(F and L)). The volume calculation in Fig. 4(F) shows a small increase between 0 and 8 Bq (8332–9119 $Å^3$) before the volume increases significantly for 16 (9938 $Å^3$) and then 20 Bq (10248 $Å^3$).

These results, combined with those reported by Rigby et al., provide stronger evidence that apo-MT adopts a relatively tight conformation, regardless of the lack of specific 2° or 3° structure. A Comparison of the Zn_7–MT and the low pH apo-βα-MT ESI-MS data is key to understanding. The low pH data show that there is a much more open structure possible, not formally a denatured structure, but one with greater oxidation exposure of the thiols. The tighter apo-βα-MT structure at neutral pH might provide some protection against oxidation and is likely the structure that metalates posttranslationally. The Bq modification data show that even modifying each cysteine does not disrupt the loosely folded structure of the metal-free protein.

These data emphasize the different descriptions of protein structure that may apply beyond the traditional descriptions. For metallothioneins, the metalated form is an example of metal-induced folding – the covalent M-S_{CYS} bonds establish the complete structural properties. For partial metalation there is ambiguity in the location of the metals – particularly in terms of the occupation of specific binding sites.

In conclusion, the ESI-MS data demonstrate that even when all cysteines in the isolated fragments and the full apo-MT are modified by Bq, MT adopts a tight configuration with a volume similar to that of the fully metallated form.

Acknowledgments

We acknowledge financial support from the Natural Sciences and Engineering Research Council (DG and RTI grants), Academic Development Grant at U.W.O. and thank Doug Hairsine for technical support with the mass spectrometer. We thank the USRA program of NSERC for summer student scholarships to A.M .and M.D (ICE scholars). We also thank Fujitsu Poland for providing the latest versions of Scigress.

References

[1] M. Margoshes, B.L. Vallee, A cadmium protein from equine kidney cortex, J. Am. Chem. Soc. 79 (1957) 4813.
[2] D.R. Winge, K.B. Nielson, Formation of the metal-thiolate clusters of rat liver metallothionein, Environ. Health Perspect. 54 (1984) 129–133.
[3] D.E.K. Sutherland, M.J. Stillman, Noncooperative cadmium(II) binding to human metallothionein 1a, Biochem. Biophys. Res. Commun. 372 (2008) 840–844.
[4] L.T. Jensen, J.M. Peltier, D.R. Winge, Identification of a four copper folding intermediate in mammalian copper metallothionein by electrospray ionization mass spectrometry, J. Biol. Inorg. Chem. 3 (1998) 627–631.
[5] A.J. Zelazowski, M.J. Stillman, Silver binding to rabbit liver zinc metallothionein and zinc alpha and beta fragments. Formation of silver metallothionein with silver(I):protein ratios of 6, 12, and 18 observed using circular dichroism spectroscopy, Inorg. Chem. 31 (1992) 3363–3370.
[6] S. Saito, M. Kurasaki, Gold replacement of cadmium, zinc-binding metallothionein, Res. Commun. Mol. Pathol. Pharmacol. 93 (1996) 101–107.
[7] A.E. Funk, F.A. Day, F.O. Brady, Displacement of zinc from metallothionein by cadmium and by mercury, Fed. Proc. 42 (1983). 1897-1897.
[8] K.T. Suzuki, T. Maitani, Metal-dependent properties of metallothionein-replacement invitro of zinc in zinc-thionein with copper, Biochem. J. 199 (1981) 289–295.
[9] K.E. Rigby, M.J. Stillman, Structural studies of metal-free metallothionein, Biochem. Biophys. Res. Commun. 325 (2004) 1271–1278.
[10] K.E. Rigby, J. Chan, J. Mackie, M.J. Stillman, Molecular dynamics study on the folding and metallation of the individual domains of metallothionein, Proteins 62 (2006) 159–172.
[11] K.E.R. Duncan, T.T. Ngu, J. Chan, M.T. Salgado, M.E. Merrifield, M.J. Stillman, Peptide folding, metal-binding mechanisms, and binding site structures in metallothioneins, Exp. Biol. Med. 231 (2006) 1488–1499.
[12] K.E.R. Duncan, M.J. Stillman, Metal-dependent protein folding: metallation of metallothionein, J. Inorg. Biochem. 100 (2006) 2101–2107.
[13] J. Chan, Z. Huang, I. Watt, P. Kille, M.J. Stillman, Characterization of the conformational changes in recombinant human metallothioneins using ESI-MS and molecular modeling, Can. J. Chem. 85 (2007) 898–912.
[14] M.E. Merrifield, Z. Huang, P. Kille, M.J. Stillman, Copper speciation in the α and β domains of recombinant human metallothionein by electrospray ionization mass spectrometry, J. Inorg. Biochem. 88 (2002) 153–172.
[15] J. Chan, Z. Huang, M.E. Merrifield, M.T. Salgado, M.J. Stillman, Studies of metal binding reactions in metallothionein by spectroscopic, molecular biology, and molecular modeling techniques, Coord. Chem. Rev. 233–234 (2002) 319–339.
[16] J.M. Snell, A. Weissberger, The reaction of thiol compounds with quinones, J. Am. Chem. 61 (1939) 450–453.
[17] B.A. Messerle, A. Schaffer, M. Vasak, J.H. Kagi, K. Wuthrich, Comparison of the solution conformations of human [Zn7]-metallothionein-2 and [Cd7]-metallothionein-2 using nuclear magnetic resonance spectroscopy, J. Mol. Biol. 225 (1992) 433–443.
[18] A.H. Robbins, D.E. McRee, M. Williamson, S.A. Collett, N.H. Xuong, W.F. Furey, B.C. Wang, C.D. Stout, Refined crystal structure of Cd, Zn metallothionein at 2.0 Å resolution, J. Mol. Biol. 221 (1991) 1269–1293.
[19] J.D. Otvos, I.M. Armitage, Structure of the metal clusters in rabbit liver metallothionein, Proc. Natl. Acad. Sci. USA 77 (1980) 7094–7098.
[20] W. Braun, M. Vasak, A.H. Robbins, C.D. Stout, G. Wagner, J.H. Kagi, K. Wuthrich, Comparison of the NMR solution structure and the X-ray crystal structure of rat metallothionein-2, Proc. Natl. Acad. Sci. USA 89 (1992) 10124–10128.

[21] D.T. Jiang, S.M. Heald, T.K. Sham, M.J. Stillman, Structures of the cadmium, mercury, and zinc thiolate clusters in metallothionein: XAFS study of Zn_7–MT, Cd_7–MT, Hg_7–MT, and Hg_{18}–MT formed from rabbit liver metallothionein 2, J. Am. Chem. Soc. 116 (1994) 11004–11013.
[22] Z. Gui, A.R. Green, M. Kasrai, G.M. Bancroft, M.J. Stillman, Sulfur K-Edge EXAFS studies of cadmium-, zinc-, copper-, and silver-rabbit liver metallothioneins, Inorg. Chem. 35 (1996) 6520–6529.
[23] J. Chan, M.E. Merrifield, A.V. Soldatov, M.J. Stillman, XAFS spectral analysis of the cadmium coordination geometry in cadmium thiolate clusters in metallothionein, Inorg. Chem. 44 (2005) 4923–4933.
[24] A. Presta, D.A. Fowle, M.J. Stillman, Structural model of rabbit liver copper metallothionein, J. Chem. Soc. Dalton Trans. (1997) 977–984.
[25] A. Presta, A.R. Green, A. Zelazowski, M.J. Stillman, Copper-binding to rabbit liver metallothionein-formation of a continuum of copper(I)-thiolate stoichiometric species, Eur. J. Biochem. 227 (1995) 226–240.
[26] M.J. Stillman, Metallothioneins, Coord. Chem. Rev. 144 (1995) 461–511.
[27] R. Grandori, Origin of the conformation dependence of protein charge-state distributions in electrospray ionization mass spectrometry, J. Mass Spectrom. 38 (2003) 11–15.
[28] L. Testa, S. Brocca, R. Grandori, Charge-surface correlation in electrospray ionization of folded and unfolded proteins, Anal. Chem. 83 (2011) 6459–6463.
[29] M. Peschke, U.H. Verkerk, P. Kebarle, Prediction of the charge states of folded proteins in electrospray ionization, Eur. J. Mass Spectrom. 10 (2004) 993–1002.
[30] P. Kebarle, A brief overview of the present status of the mechanisms involved in electrospray mass spectrometry, J. Mass Spectrom. 35 (2000) 804–817.
[31] C.A. Blindauer, N.C. Polfer, S.E. Keiper, M.D. Harrison, N.J. Robinson, P.R.R. Langridge-Smith, P.J. Sadler, Inert site in a protein zinc cluster: isotope exchange by high resolution mass spectrometry, J. Am. Chem. Soc. 125 (2003) 3226–3227.
[32] G. Acampora, J. Hermans Jr., Reversible denaturation of sperm whale myoglobin. Dependence on temperature, pH, and composition, J. Am. Chem. 89 (1967) 1543–1547.
[33] J. Chan, Z. Huang, I. Watt, P. Kille, M.J. Stillman, Metallobiological necklaces: mass spectrometric and molecular modeling studying of metallation in concatenated domains of metallothionein, Chem. Eur. J. 14 (2008) 7579–7593.
[34] D.E.K. Sutherland, K.L. Summers, M.J. Stillman, Noncooperative metalation of metallothionein 1a and its isolated domains with zinc, Biochemistry (2012), http://dx.doi.org/10.1021/bi3004523.
[35] M.F. Sanner, NIH calculator, The Scripps Research Institute, La Jolla, California, 1996 <http://mgl.scripps.edu/people/sanner/html/msms_man.html>.
[36] T.T. Ngu, A. Easton, M.J. Stillman, Kinetic analysis of arsenic - Metalation of human metallothionein: Significance of the two-domain structure, J. Am. Chem. Soc. 130 (2008) 17016–17028.